J Mater Sci (2009) 44:5485–5493
DOI 10.1007/s10853-009-3766-3

The fabrication of a MWNTs–polymer composite chemoresistive sensor array to discriminate between chemical toxic agents

Chang-Pin Chang · Chun-Lung Yuan

Received: 4 March 2009 / Accepted: 18 July 2009 / Published online: 29 July 2009

Abstract In this study, a chemoresistive sensor was fabricated by the chemical polymerization and coating of either polyaniline (PANI), poly[2-methoxy-5-(2-ethyloxy)-*p*-phenylenevinylene], or commercial poly(methyl methacrylate) on MWNTs. We investigated the resistance responsiveness of the multilayer samples to simulated chemical warfare agents, including dimethyl methyl phosphonate (DMMP) and dichloromethane (DCM), as well as to organic agents, such as chloroform, tetrahydrofuran, methyl-ethyl ketone, and xylene. The MWNTs–PANI film was characterized by SEM and FT-IR, and the resistivity values for the six solvents were measured at different temperatures. We observed that the MWNTs-PANI sensing film exhibited a high sensitivity, excellent selectivity, and good reproducibility to the detection of all of the aforementioned agent vapors. In addition, we used atomic force microscopy to demonstrate the MWNTs–PANI absorption of DMMP vapor, wherein the sensing film exhibited a swelling phenomenon, such that the film thickness increased from 0.8 to 1.3 μm. In addition, we used principal component analysis to evaluate the performance of the sensor in detecting DMMP, DCM, and the aforementioned organic agent vapors.

C.-P. Chang (✉)
Department of Applied Chemistry & Materials Science, Chung Cheng Institute of Technology, National Defense University, No 190, Sanyuan 1st St. Dahsi, Jen, Taoyuan 335, Taiwan
e-mail: junelong@mail2000.com.tw; g990202@gmail.com

C.-L. Yuan
Graduate School of Defense Science, Chung Cheng Institute of Technology, National Defense University, No 190, Sanyuan 1st St. Dahsi, Jen, Taoyuan 335, Taiwan

Introduction

Organic chemical agents are colorless, toxic, and very harmful to human health and the environment. These agents usually exist as liquids, but their vapors can be inhaled or absorbed through the skin. Fast and accurate detection of chemical agents is essential for protecting human health [1]. Contemporary sensors used to detect these gases include metal oxide semiconductors, colorimetric indicators, quartz-crystal microbalance sensors, electrochemical/chemical polymer nanostructure sensors, and surface acoustic wave sensors [2–6]. Unfortunately, adaptive sensor in a complex gas environment for selectivity is still an urgent problem.

"Nanostructured polymer" detectors for chemical warfare agents and toxic industrial chemical reagents must be portable, fast-acting, inexpensive, simple to operate, sensitive, and selective. In recent years, many studies investigated polyaniline (PANI), which exhibits excellent environmental stability in its conducting form, and its potential application to various fields, such as solar energy conversion, electronic magnetic shielding, and sensing [7]. Anitha et al. have demonstrated the recognition and exposing of intermolecular interaction between CH_2Cl_2 and $CHCl_3$ using PANI [8].

Carbon nanotubes were discovered in 1991[9], and have since received considerable interest for their potential use in the fabrication of new classes of advanced materials due to their unique properties. Carbon nanotubes have been investigated for use in polymeric materials, wherein they improve the mechanical properties of composites and electrically conducting devices. In comparison to the aforementioned contemporary sensors, MWNTs–polymer composite sensors have many advantages, such as high sensitivity, fast response, good reproducibility, and long-term stability [10, 11].

In this study, we analyzed the gas identification ability of layered MWNTs–polymer sensors. These sensors were designed to reversibly swell, which causes resistance changes upon exposure to a wide variety of chemical warfare and organic agents with gas/vapor concentrations at ppm levels. Until now, there has been extensive theoretical investigation of the interaction between polymers and MWNTs, but without experiments demonstrating the theoretical.

In our tests, we used dimethyl methyl phosphonate (DMMP) to simulate a nerve agent and dichloromethane (DCM) as a choking agent. The organic agents chloroform ($CHCl_3$), tetrahydrofuran (THF), methyl-ethyl ketone (MEK), and xylene were also tested. To investigate the swelling process, we analyzed the adsorption kinetics of the film using atomic force microscopy (AFM). Principal component analysis (PCA) was used as one of the statistical classification methods to classify the six test gases.

Experimental

Materials

MWNTs were produced by chemical vapor deposition with a nominal outside diameter (OD) of 30–40 nm. PANI and poly[2-methoxy-5-(2-ethyloxy)-*p*-phenylenevinylene] (MEH-PPV) were prepared in our laboratory [12, 13]. Poly(methyl methacrylate) (PMMA) was purchased from CHI MEI Corporation Co., Taiwan. All the chemical agents used (DCM, THF, $CHCl_3$, MEK, xylene, 1-methyl-2-pyrrolidone, and sodium dodecylbenzenesulfonate) were of Analysis reagent grade. DMMP was purchased from Tokyo Chemical Industry Co., Ltd., and distilled before use.

Preparation of thin film (multilayer)

The first MWNTs (1 wt%) layer-modified electrode was prepared by drop-casting 1 mg/mL MWNTs dissolved in MEK as a dispersion on the surface of a interdigitated microelectrode (IME) device, which was then air-dried at room temperature. When the MEK evaporated, a MWNTs film was formed. The polymer film was deposited by these solutions (1 wt% MEH-PPV, PMMA, or 1 wt% PANI ultrasonicating for 10 min) being drop-cast onto the MWNTs layer. After vacuum-drying, the multilayer films were formed. The functionalized MWNTs–PANI samples were characterized using several techniques. A Fourier transform infrared (FT-IR, Brucher VECTOR22 spectrometer of Varian) spectrometer was used to examine the types of functional groups present on those samples. The observation of PANI, MWNTs, and PANI–MWNTs morphology was performed by a JSM-6500F scanning electron microscope (SEM).

Sensor measurements and characterization

Sensor response was measured using a customized IME device, which has 12 pairs of 1-mm wide gold electrodes, spaced 1 mm apart, on a SiO_2 wafer substrate (Fig. 1).

A computer-interfaced multichannel multimeter (in house) was used to measure the lateral resistance of the nanostructured coating on the IME. Resistance and frequency measurements were simultaneously performed with computer control. All experiments were performed at different temperatures (30, 40, and 50 °C). The analyte vapor gas flow was controlled by a calibrated Aalborg mass-flow controller (GFM-17), wherein the flow rate of the vapor stream was maintained at 100 mL/min. The vapor-generating system relied on the Gas Standard Generator (KINTEK, Laboratories. Inc., 670C.). The vapor stream was produced by drying of the vapor solvent and using the controller to manipulate vapor concentration. We measured the $R\%$ and used the relative differential resistance change, $\Delta R/R_{air}$, to evaluate the responses of the sensors to the vapors. The value ΔR is the difference between the maximum values of the resistance response, whereas R_{air} is the initial resistance of the film. The IME devices were housed, and connected via tubing to the vapor and air pump sources in a Teflon chamber (inner diameter of 1/8 inch). The vapor concentration (ppm) in the unit was calculated from the weight loss and volume of analyte at different temperatures (see Table 1), which can be expressed as in Eq. 1:

$$\text{Conc.} = (R \times K)/F \quad (\text{v/v in ppm}), \tag{1}$$

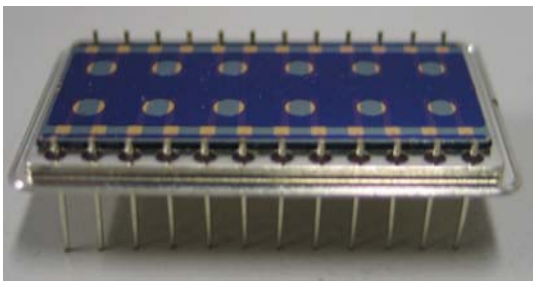

Fig. 1 The configuration of IMEs

Table 1 Concentration (ppm) of the six chemical agent vapors

Temperature (°C)	DMMP ppm	Xylene	$CHCl_3$	THF	DCM	MEK
30	332	839	2,238	6,795	481	1,045
40	747	839	3,283	8,363	962	1,853
50	797	855	4,850	9,768	1,442	3,136

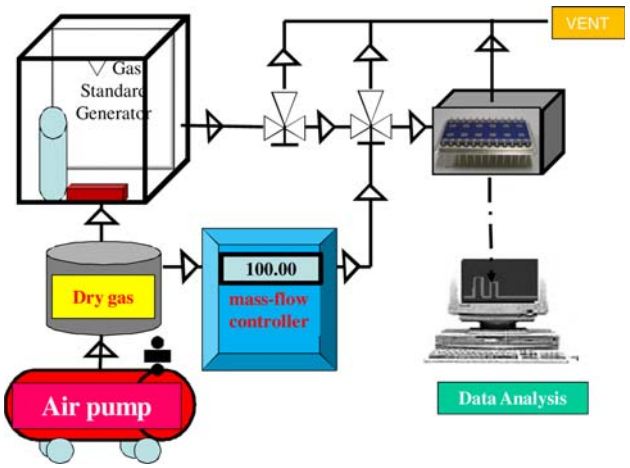

Fig. 2 Resistance measurement instrument

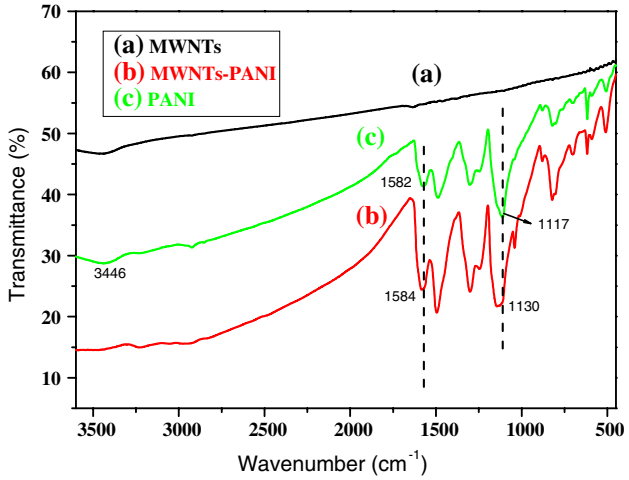

Fig. 3 FTIR spectra of (*a*) MWNTs, (*b*) MWNTs–PANI, and (*c*) pure PANI

where $K = \{22.4(T + 273) \times 760\}/\mathrm{MW} \times 273 \times P$, R (mg/min) is the weight loss for analyte, and F (mL/min) is the flow ratio.

Figure 2 depicts the resistance measurement apparatus. Air was used as the gas carrier. Different concentrations of vapors were generated by an impingement system. At the beginning of the experiment, the test chamber was purged with air for 30 min to ensure the absence of air and to establish a baseline. For the experiment, the chamber was purged with air for 10 min and then the test vapor at the desired concentration for 5 min.

Surface absorption swelling was investigated using a Nanoscope IIIa (Digital Instruments) AFM to produce 256 × 256 pixel images under ambient conditions in tapping model. The average height and diameter of the film were determined using the software from Digital Instruments.

Results and discussion

FT-IR

Figure 3 depicts the FT-IR spectra of MWNTs, PANI, and MWNTs–PANI composites. The characteristic absorption band of PANI is 1582 cm^{-1} (N=Q=N) and 1117 cm^{-1} (C–N) (Fig. 3c), whereas the absorption peaks of MWNTs–PANI composites shifted to 1584 and 1130 cm^{-1} (see Fig. 3b). The absorption peak of composite with MWNTs–PANI shifted about 2 and 13 cm^{-1} when compared to that of the pure PANI. These results indicate that there are some degree of intermolecular interaction between MWNTs and PANI. As shown in Fig. 3a, the pure MWNTs will not show any peak appearing between 2000 and 600 cm^{-1} absorption.

Scanning electron micrographs

Scanning electron micrographs (SEM) of the MWNTs and PANI are shown in Fig. 4. In these micrographs, PANI can be seen as an amorphous region. The surface of the particles is not smooth; lumps and holes (about 100 nm) in the material can be seen (Fig. 4a). This uneven surface is a good property for gas adsorptions. As shown in Fig. 4b, the SEM images also reveal that the MWNTs, with a diameter ranging from 30 to 80 nm, are well distributed on the surface and that most of the MWNTs are in the form of small bundles or single tubes. Such small bundles and single tubes assembled homogeneously on the substrate are believed to benefit sensor performance because most of the well-dispersed MWNTs are electrochemically accessible. In contrast, Fig. 4c shows that depositing PANI on MWNTs film produces a multilayer morphology, where holes on the surface of the film and agglomeration were also observed. The larger diameter of PANI covering MWNTs compared to the neat MWNTs is visible. The anchoring of PANI covering the MWNTs surface can impart its compatibility and transfer the electron, which greatly improves responsiveness and reversibility of the materials.

Gas-sensing resistivity behavior

The resistance characteristics in DCM vapor of MWNTs–PANI and pristine PANI films are shown in Fig. 5. The approximately linear relationship that is seen suggests that no sensitivity have been established in the pristine PANI polymer film using IMEs (see Fig. 5a). Figure 5b shows the response curves of MWNTs–PANI conductivity film for sensitivity percentage, which was approximately 8%.

This dramatic change in sensitivity is attributed to the anchoring of the PANI to the MWNTs surface, which

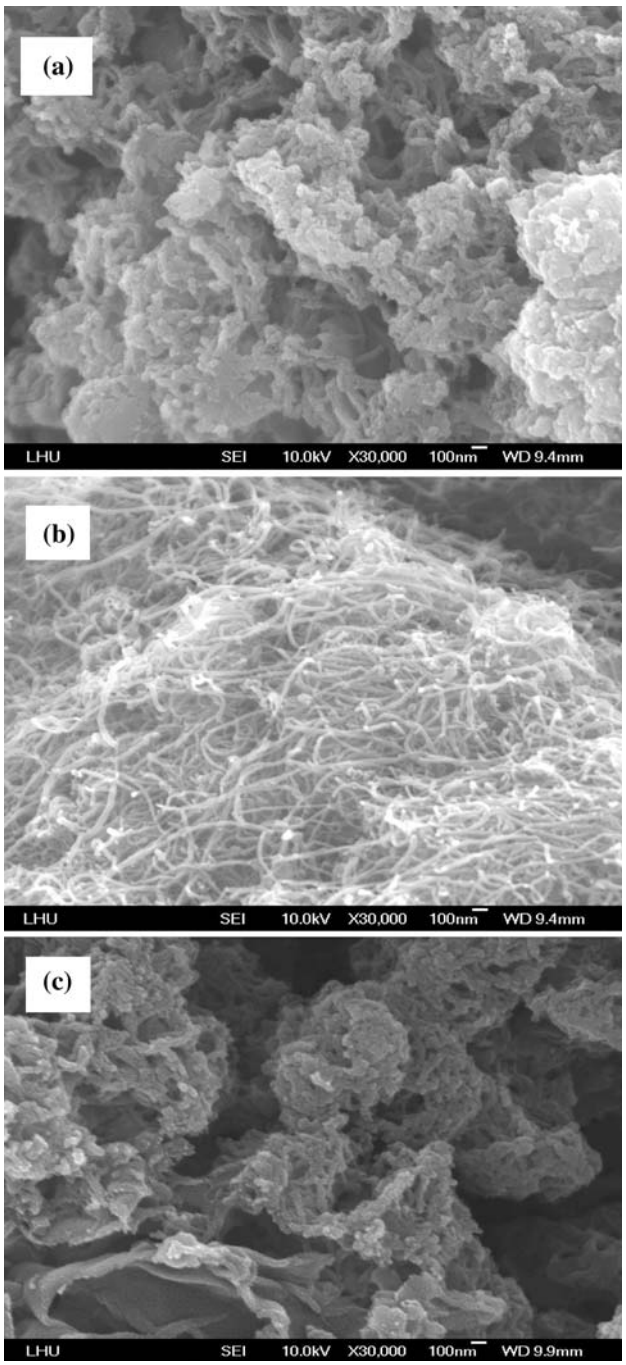

Fig. 4 SEM images of (**a**) pure PANI, (**b**) MWNTs, and (**c**) MWNTs–PANI

imparts its compatibility, and the MWNTs primarily act as a conduction pathway from the matrix to IMEs used to increase the conductivity of the material. So, the MWNTs–PANI polymer film greatly improves the responsiveness and reproducibility of the materials.

Additionally, we carried out consecutive response studies of the three MWNTs–polymers sensing films of repeated exposures to DCM vapor. One of the important

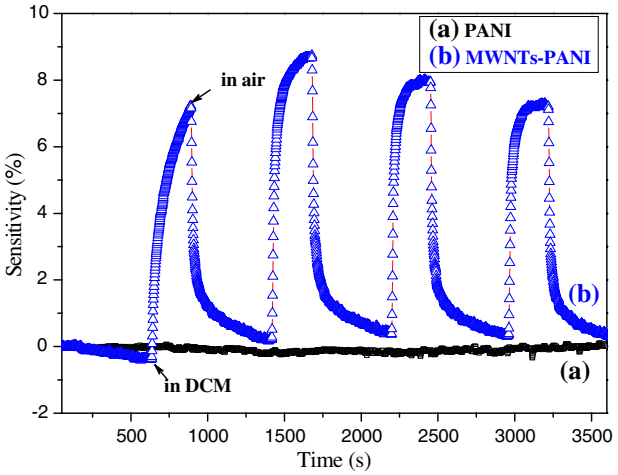

Fig. 5 The sensitivity responses comparison between (*a*) PANI and (*b*) MWNTs–PANI films in DCM vapor

characteristics of the sensors, in addition to selectivity and sensitivity, is its ability for regeneration. Figure 6 shows the difference response patterns of the sensors based on the MWNTs–PANI, MWNTs–PMMA, and MWNTs–MEH-PPV composites. The sensitivity of the MWNTs–PANI sensing film drastically increased by over about 7 orders of magnitude within 200 s after exposure to 1442 ppm DCM vapor. When the MWNTs–PANI film was transferred from the solvent vapor into dry air, the resistance rapidly returned to the original value of 396 s, showing a very large improvement in restoring performance and about 30 min after obvious stability (see Fig. 6a). However, Fig. 6b showing the MWNTs–MEH-PPV and MWNTs–PMMA sensing films failed to exhibit noticeable sensitivity changes after 250 s exposure to DCM vapor and increased about 1.9 and 0.7 orders of magnitude, respectively. Thus, a highly selective chemical gas sensor based on MWNTs with PANI can be obtained.

In addition, we compared the response of the three MWNTs–polymer composite sensing films to six solvent vapors. The time dependence of the changes in the normalized resistance for the three MWNTs–polymers exposed to vapors of DMMP, DCM, THF, $CHCl_3$, MEK, and xylene are depicted in Fig. 7. All three systems exhibit a highest response intensity or responsivity to DMMP vapor, implying that MWNTs–PANI's excellent responsiveness is due to the nature of the PANI matrix itself. Herein, we define the relative sensitivity responsiveness as

$$\Delta R = \log[(R_{\text{gas}} - R_{\text{air}})], \tag{2}$$

where R_{air} is the original resistance and R_{gas} is the maximum resistance of the film upon exposure to the simulated chemical warfare and organic solvent vapors.

It can also be seen in Fig. 7 that the responsivities of the MWNTs–PANI system for DMMP, DCM, THF, $CHCl_3$,

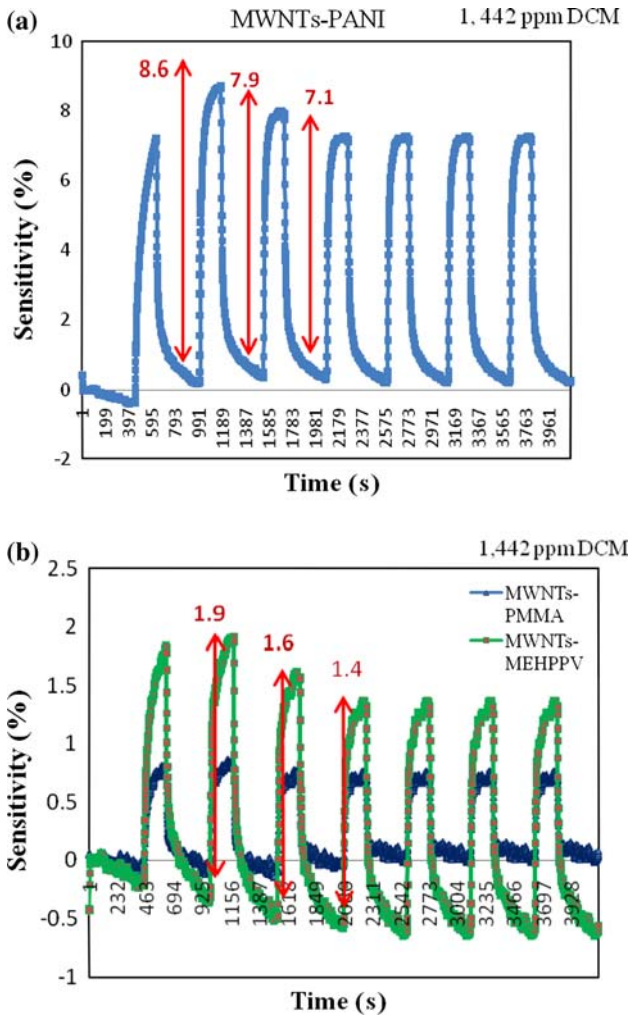

Fig. 6 Typical electrical responses of (**a**) MWNTs–PANI and (**b**) MWNTs–MEH-PPV, MWNTs–PMMA films to 1442 ppm DCM vapor

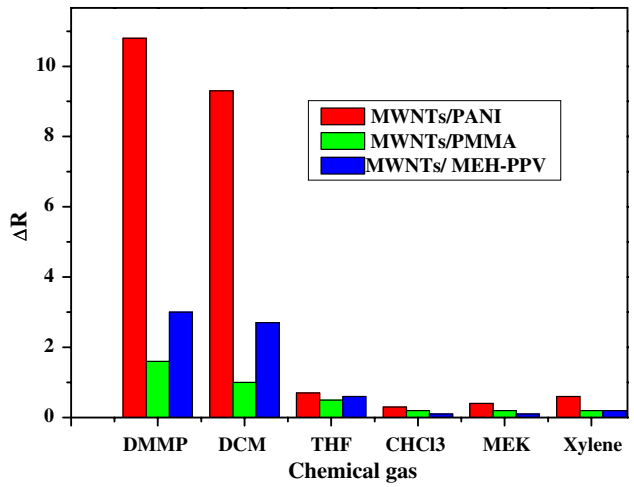

Fig. 7 Relative resistance responsivity of MWNTs–polymer sensing films against various chemical vapors at 50 °C

MEK, and xylene under 50 °C exposures are approximately 10.8, 8.6, 0.7, 0.3, 0.4, and 0.6, respectively. However, only very small responsivities to any other solvent vapors were observed, and the film did not respond to nonpolar solvent vapors, for example, MEK. These data indicate that the MWNTs–PANI sensor has a strong anti-jamming ability and a high sensitivity to DCM and DMMP vapors, and we consider it to be an ideal candidate for selective sensing.

The difference in response between the MWNTs–PMMA and MWNTs–MEH-PPV composites exposed to the six aforementioned agents (see Fig. 7) clearly shows a responsivity of 6 and 8 orders of magnitude higher than that of the MWNTs-MEH-PPV and MWNTs-PMMA films, respectively, to DMMP and DCM vapors.

Absorption/stripping mechanism of gas-sensing behavior

According to absorption/stripping, the response mechanism may be associated with the differences in the physical adsorption properties of the MWNTs and polymers for different organic chemical vapors. A high polar surface energy component was observed for MWNTs, which is significantly different from that of a carbon black particle [14], leading to different interactions between the MWNTs and the polymers. Moreover, the layered MWNTs–polymer composites have central hollow core structures, which permit analytes to permeate the MWNTs–polymer film from both the inner and outer layers, thus permitting the polymers to rapidly swell. Additionally, it is likely that when interlayer interactions between carbon nanotubes are introduced, the MWNTs–polymer can be induced to change from metal-like to semiconductor-like, resulting in an increase in resistance. Of course, whether DMMP can induce a change in conductive performance by adsorption on the MWNTs–PANI surface still requires further study. This structure facilitates the formation of intra- and intermolecular hydrogen bonds [15], wherein electronic transitions from the valance band to the mid-band gap states occur when the polaron state contains one electron and the bipolaron state is completely empty (i.e., contains two holes).

In this case, polymeric "swelling" and "shrinking" destroys the original structure or configuration of the film. At the same time, the volume of polymer increases when it swells, and the interlayer distance between MWNT increases, breaking the conducting network and leading to a large increase in the electrical resistance of the film. It is worth noting that the swelling behavior of polymer chains wrapped around MWNTs is very different from that of a pure polymer matrix. The former involves the influence of the interactions on the surface of the MWNTs–polymer

[16], while the interaction among the polymer chains differs in the latter case, since aggregation occurs more easily. Thus, the shrinking ability of the polymer alone is not sufficient to explain the aforementioned phenomenon. Until now, there has been no extensive investigation of the absorption kinetics for the interaction between polymers and MWNTs. One viewpoint has suggested that the polymer molecular structure and atomic interactions at carbon nanotube interfaces can significantly influence the properties of the sensor system [17]. Another viewpoint has suggested that the weak electrostatic or noncovalent interactions between the highly delocalized electron systems of the carbon nanotube and the polymer may affect the molecular recognition ability of solvent molecules by PANI. For covalently functionalized MWNTs, the polymer chains are individually anchored onto the tube surface, forming a nanoscale layer of coverage (where the thickness is dependent on the amount of polymer), especially in the case of higher conducting polymer proportions between MWNTs. A hopping mechanism is responsible for intertube charge transfer between the carbon nanotubes and the intertube modulation of the carbon nanotubes network in lieu of a conductivity change [18].

In this work, the absorbefacient mechanism of PANI swelling after exposure to DMMP analytes was observed with AFM. AFM images were taken of the vacuum-dried MWNTs–PANI sensitive layer, which involved a combination of both PANI and multiwalled carbon nanotubes with a 1 μL consistence. Geometric diagrams at a scale of $10 \times 10\ \mu m^2$ and scan rate 0.5 Hz are shown in Fig. 8. The greatest amount of absorbent was obtained at this time, as described previously. Cross-sectional analysis of DMMP vapor was able to distinguish the growth direction of MWNTs–PANI. Prior to exposure to an absorbing gas, an aggregation of grains on the MWNTs surface was observed, and the maximum height of the grains was approximately 818 nm, with a root-mean-square (RMS) roughness of 0.8 μm. After exposure to DMMP gas for 5 min, the range of heights varied from 818 nm to 1.8 μm, and the RMS roughness increased from 0.8 to 1.3 μm on the MWNTs–PANI film. These results may reveal that the MWNTs–PANI sensitivity has an important role when gas passes spontaneously through the coated surface. The detailed mechanism of the AFM formation of the MWNTs–PANI sensing film exposure to DMMP was not clear, and should be extensively studied in the future.

MWNTs–PANI gas-sensing sensitivity behavior

In our study, although $CHCl_3$ is as good a polar solvent for MWNTs–polymer films, it does not induce a good resistivity response. On the other hand, the simulated chemical warfare agents DMMP and DCM clearly induce excellent responses. DMMP vapor molecules are especially good agents for the MWNTs–PANI film. DMMP has strong electron donor properties, and therein, the sensor adsorption of

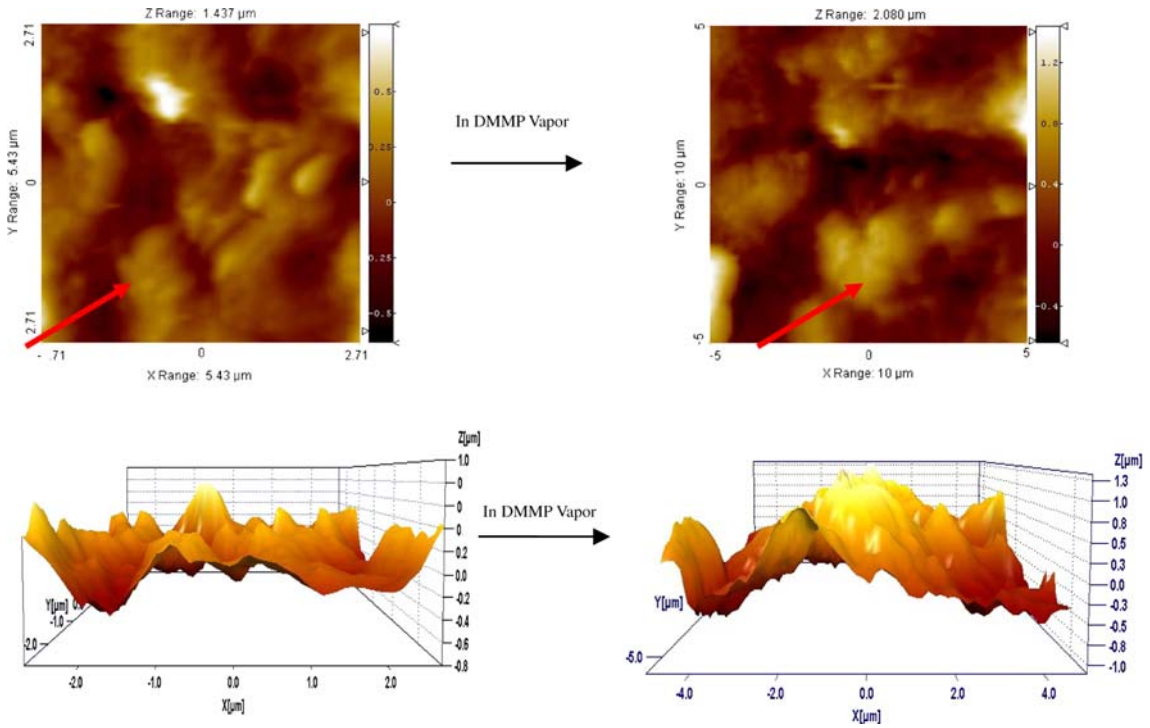

Fig. 8 AFM images of MWNTs–PANI sensing film adsorption of DMMP for 5 min

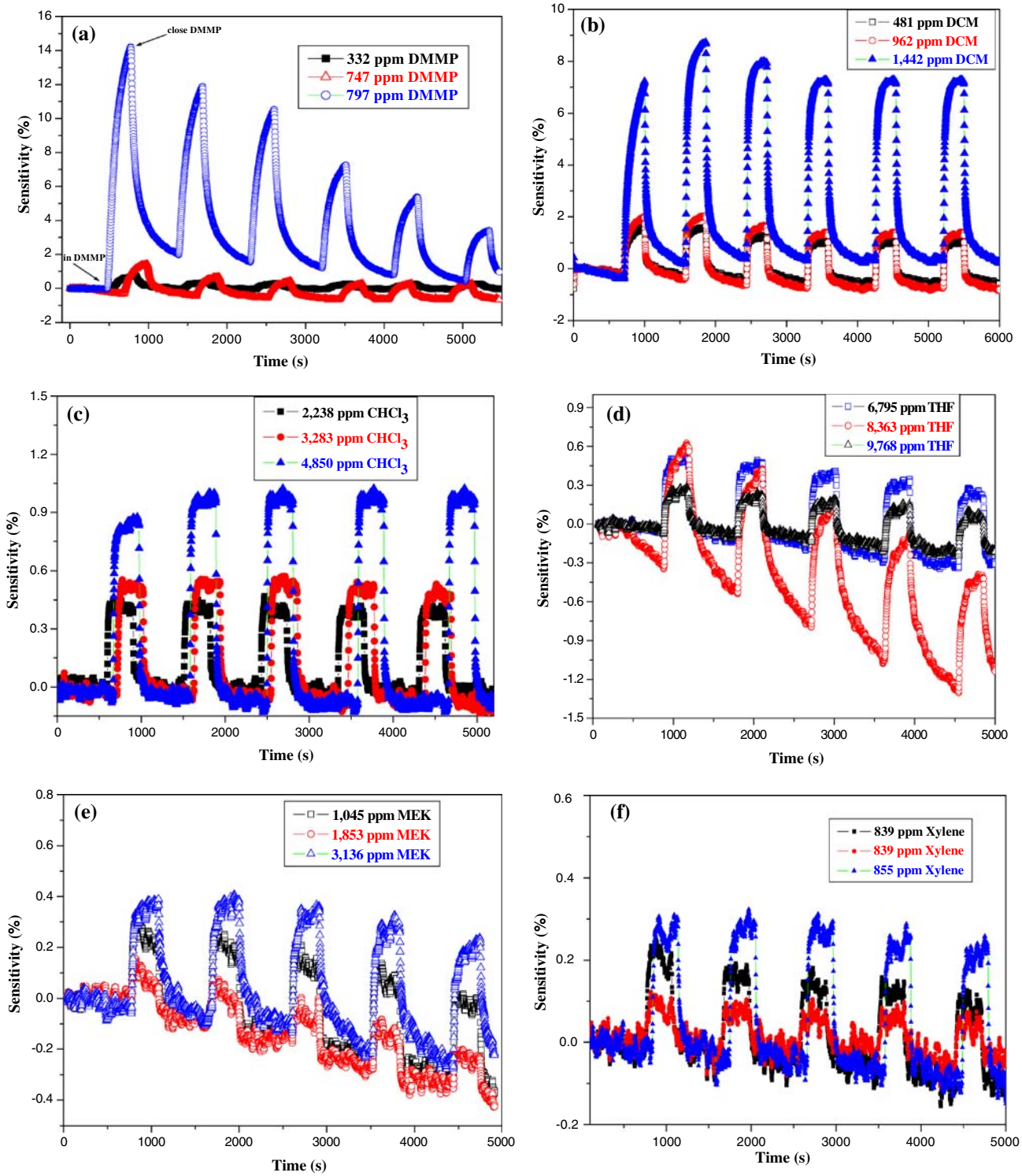

Fig. 9 Reproducibility of MWNTs–PANI sensing films sensitivities for simulated chemical warfare agent and organic agents' vapors

a DMMP agent results in a partial charge transfer between the analyte and MWNTs–PANI that changes its electrical resistance and speeds up the motion and swelling of the polymer chains; it thereby breaks the conductive path and leads to an increase in resistance.

Good reproducibility and long-term stability are important parameters for a gas sensor material. Figure 9 clearly shows that the sensors fabricated from the three MWNTs–PANI sensing films device exhibit better resistance reproducibility and stability after 5–6 times cycles of exposure

to chemical agent vapors and dry air. Here, the relative sensitivity responsiveness is defined as

$$S\% = [R/R_0] \times 100\%, \quad (3)$$

where R_0 is the resistance of sample at dry air and R is the resistance when it is exposed to the target gas. Figure 9a and b clearly shows that the sensitivity of the MWNTs–PANI sensing film drastically increased by 14.17 and 7.4% within 290 s of exposure to 50 °C DMMP and DCM vapors, respectively. When the film was transferred from the solvent vapor into dry air, the electrical resistance rapidly returned to the original value, demonstrating a good restoring performance. We attribute this behavior to the weak hydrogen bond interaction between the $CHCl_3$ vapor and the polymer, which can result in a rapid adsorption of analyte molecules (Fig. 9c). These results further suggest that the sensing films response is fast, reversible, and reproducibility. Therefore, a highly selective organic solvent gas sensor based on MWNTs–PANI was obtained. Over a period of 5000 s, the maximum variation in the baseline resistivity was less than 4%. In contrast, obtain standard error value by absorbing resistance value of 3 times of simulate warfare agents (DCM, DMMP) observed in the ranges between 1.4×10^{-1}–7.3×10^{-1} and 1.8×10^{-1}–7.9×10^{-2} in Fig. 10a, and all organic agents observed in the ranges 8.3×10^{-2}–6.5×10^{-3} in Fig. 10b, so as to establish the polymer sensing films and detect the chemical vapors under different temperature. Such minor shifts did not significantly affect the response pattern and applicability of the sensors. These results imply that the MWNTs–PANI material exhibits excellent selectivity, and is therefore a very promising candidate for vapor sensing applications.

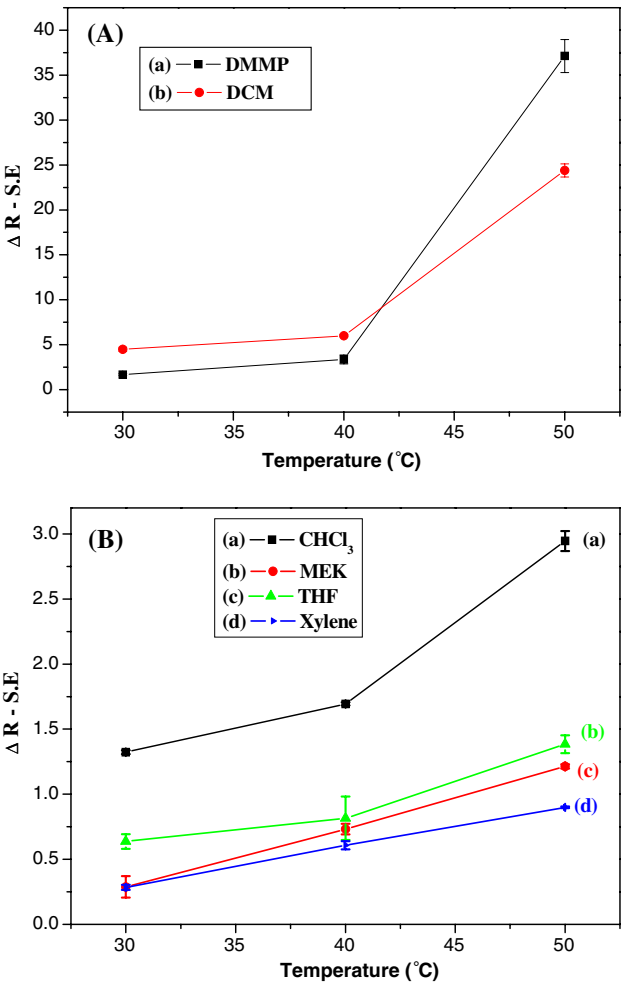

Fig. 10 Standard error value of MWNTs–PANI sensing films sensitivities for simulated chemical warfare agents and organic agents' vapors

PCA statistical method

The PCA statistical method was applied to the signal of the optimized sensor array, and the input data from the primary matrix were the normalized responses, which were chosen to represent the relative resistance change ($\Delta R/R_0$) of the MWNTs–polymer sensors. The PCA data obtained by the correlation matrix (centered and standardized data) [19]. The responses of the three MWNTs–polymer sensors were normalized by the sum of all the sensor response values for a given analyte. This normalization process reduced the dependence of the array response on the vapor concentration and also slightly reduced the effects of sensor drift. Figure 11 depicts the score plot in the PC_1–PC_2 class plane of six distinct clusters of DMMP, DCM, THF, $CHCl_3$, MEK, and xylene plus a spread of data points related to organic agents with different graduated mixing ratios. The fact that PC_1–PC_2 separate regions included the measurement of a single simulator indicates that two different simulator in the same test can be clearly discerned from one another. Between the 6 dots of DMMP, DCM, THF, $CHCl_3$, MEK, and xylene, as indicated in Fig. 11, another evolved region of organic agents can be fixed in the feature plane analyzed (PC_1–PC_2) with a high cumulative variance exceeding over 99.728%. As previously noted, the largest portion of the variance was included in the first principal component (PC_1), which is also the most important in the discrimination of the dot. The second principal component (PC_2) contained less information (0.235%), while the third principal component included the least amount of variation (0.036%). Table 2 shows the total and percentage eigenvalue variance for the extracted principal components. The minimal eigenvalue was set to 0.020, and the first three principal components were calculated. The information content of the third eigenvalue was 0.036%, corresponding to an eigenvalue of 0.020, which was below the selected limit. The information content of the second eigenvalue was 0.235%, corresponding to an eigenvalue of 0.129,

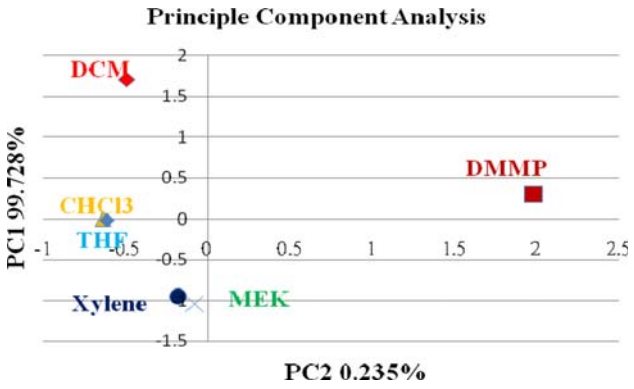

Fig. 11 PCA score plot of DMMP, DCM, and organic agents in the PC_1–PC_2 plane of the original dataset obtained from the normalized responses of the all three different MWNTs–polymer sensors of the IME

Table 2 Percentage variance according to the PCA analysis performed on the correlation matrix of the primary data associated with the normalized responses of the three sensors

Principal components	Eigenvalue		
	Total	Variance (%)	Cumulative variance (%)
1	55.054	99.728	99.728
2	0.130	0.235	99.964
3	0.020	0.036	100.00

which was above the selected limit. The remaining variance (0.036%) in the third principal component represented only noise in the primary data matrix; the most significant information was contained in the first two principal components (99.964% cumulative variance). We can conclude that there were no redundant sensors in the studied array.

Conclusion

We have demonstrated that the chemical polymerization and coating of three polymers on the surface of MWNTs can produce remarkable gas sensing properties for the detection of the chemical simulant agents DMMP and DCM as well as the organic agents $CHCl_3$, THF, MEK, and xylene. The sensitivities of the MWNTs–polymer films for the six solvents in decreasing order were MWNTs–PANI > MWNTs–MEH-PPV > MWNTs–PMMA, which corresponds to an order of decreasing conductivity. The results showed that the MWNTs–PANI sensor provided high sensitivity, excellent selectivity, good reproducibility, and long stability for all the investigated different concentration agent vapors. The modification of the electronic structure of MWNTs by chemical functionalization proved to be a valuable route to the development of an advanced sensor material. We suggest that the swelling and shrinking behavior of the polymer chains covering the MWNTs as well as the interaction between the PANI chains and analytes may play important roles in gas sensing. Changes in film resistance were caused by changes in interlayers distance, which is induced by polymer swelling upon gas absorption. In addition, AFM images depict the swelling of MWNTs–polymer composites due to vapor absorption, as theoretically predicted. The response of the MWNTs–PANI film to DCM, DMMP, $CHCl_3$, MEK, and xylene differed from that of any other polymers and solvents, which we attribute to a hydrogen bond interaction between the solvent molecules and the PANI chains. This interaction is greatly affected by the properties of the MWNTs. In summary, we have developed polymer-functionalized MWNTs sensor platforms for the detection of vapors from chemical warfare and organic agents at room temperature. We applied PCA to distinguish the performance of the as-fabricated films to DMMP, DCM, and organic agents' exposures. The devices developed in this study can potentially be further extended to MWNTs/PANI sensors for highly sensitive and specific molecular detection.

References

1. Okimura T, Takasu N, Ishimatsu S (1996) Ann Emerg Med 28:129
2. Gardner JW (1991) Sens Actuators B 4:109
3. Nakamoto T, Fukuda A (1993) Sens Actuators B 10:85
4. Nanto H, Kawai T, Sokooshi H, Usuda T (1993) Sens Actuators B 14:718
5. Lee TJ, Song HY, Chung DJ (2003) J Korean Phys Soc 42:814
6. Chung WY (2002) J Korean Phys Soc 41:181
7. Gurunathan K, Murugan AV, Marimuthu R, Mulik UP, Amalnerkar DP (1999) Mater Chem Phys 61:175
8. Anitha G, Subramanian E (2005) Sens Actuators B 107:605–615
9. Iijima S (1991) Nature 354:56
10. Wu T-M, Lin Y-W (2006) Polymer 47:3576
11. Alig I, Lellinger D, Dudkin SM, Pötschke P (2007) Polymer 48:1020
12. Chang C-P, Chao C-Y, Huang JH, Li A-K, Hsu C-S, Lin M-S, Hsieh BR, Su A-C (2004) Synth Met 144:297
13. Chang C-P, Yuan C-L, Ho C-M (2008) J Explos Propellants 24:33
14. Harris PJF (1999) Carbon nanotubes and related structures: new materials for the twenty-first century. Cambridge University Press, Cambridge
15. Matsuguchi M, Umeda S, Sadaoka Y, Sakai Y (1998) Sens Actuators B 49:179
16. Niu L, Luo Y, Li Z (2007) Sens Actuators B 126:361
17. Wei C (2006) Nano Lett 6:1627
18. Valentini L, Bavastrello V, Stura E, Armentano I, Nicolini C, Kenny JM (2004) Chem Phys Lett 383:617
19. Choi N-J, Kwak J-H, Lim Y-T, Bahn T-H, Yun K-Y, Kim J-C, Huh J-S, Lee D-D (2005) Sens Actuators B 108:298